Analysis of the $\Lambda_b \to \Lambda \ell^+ \ell^-$ decay in QCD

T. M. Aliev[a] *†, K. Azizi[b] ‡, M. Savcı[a] §

[a] Physics Department, Middle East Technical University, 06531 Ankara, Turkey

[b] Physics Division, Faculty of Arts and Sciences, Doğuş University

Acıbadem-Kadıköy, 34722 Istanbul

Abstract

Taking into account the Λ baryon distribution amplitudes and the most general form of the interpolating current of the Λ_b, the semileptonic $\Lambda_b \to \Lambda \ell^+ \ell^-$ transition is investigated in the framework of the light cone QCD sum rules. Sum rules for all twelve form factors responsible for the $\Lambda_b \to \Lambda \ell^+ \ell^-$ decay are constructed. The obtained results for the form factors are used to compute the branching fraction. A comparison of the obtained results with the existing predictions of the heavy quark effective theory is presented. The results of the branching ratio shows the detectability of this channel at the LHCb in the near future is quite high.

PACS number(s): 11.55.Hx, 13.30.-a, 14.20.Mr

*e-mail: taliev@metu.edu.tr

†permanent address:Institute of Physics,Baku,Azerbaijan

‡e-mail: kazizi@dogus.edu.tr

§e-mail: savci@metu.edu.tr

1 Introduction

Experimentally, the detection and isolation of the heavy baryons is simple comparing to the light systems since having the heavy quark makes their beam narrow. In the recent years, considerable experimental progress has been made in the identification and spectroscopy of the heavy baryons containing a heavy bottom or charm quark [1–8]. These evidences can be considered as a good signal to search also the decay channels of the heavy baryons like, $\Lambda_b \to \Lambda \ell^+ \ell^-$ at LHCb. This rare channel, induced by the flavor changing neutral currents (FCNC) of $b \to s$ transition, serves testing ground for the standard model at loop level and is very sensitive to the new physics effects [9], such as supersymmetric particles [10], light dark matter [11] and also fourth generation of the quarks and extra dimensions, etc. Moreover, this channel can be inspected as a useful tool in exact determination of the Cabibbo-Kobayashi-Maskawa (CKM) matrix elements, V_{tb} and V_{ts}, CP and T violations, polarization asymmetries.

Theoretically, there are some works devoted to the analysis of the heavy baryon decays, where practically in all of them the predictions of the heavy quark effective theory (HQET) for form factors have been used. Transition form factors of the $\Lambda_b \to \Lambda_c$ and $\Lambda_c \to \Lambda$ decays have been studied in three points QCD sum rules in [12], the $\Lambda_b \to p l \nu$ transition form factors have also been calculated via three point QCD sum rules in the context of the heavy quark effective theory (HQET) in [13] and in the framework of the SU(3) symmetry and HQET in [14]. In the present work, using the most general form of the interpolating current for the Λ_b and also the distribution amplitudes of Λ baryon, all form factors related to the electroweak penguin and weak box diagrams describing the $\Lambda_b \to \Lambda \ell^+ \ell^-$ are calculated in the frame work of the light cone QCD sum rules in full theory. The obtained results for the form factors are used to estimate the decay rate and branching ratio. Regard that this transition has been investigated in [15] and [16] also in the context of the HQET but the same frame work using the distribution amplitudes of the Λ and Λ_b, respectively. Moreover, form factors, branching ratio and di–lepton forward–backward asymmetries are studied in [17–19] also within the context of the HQET. In [20–22], $\Sigma_{b,c}$ and $\Lambda_{b,c}$ to nucleon transitions are also evaluated using the nucleon wave functions in light cone QCD sum rules approach.

The plan of the paper is as follows: in section II, the light cone QCD sum rules for the form factors are obtained using the Λ DA's. The HQET relations among all form factors are also discussed in this section. Section III is dedicated to the numerical analysis of the sum rules for the form factors as well as numerical results of the decay rate and branching ratio.

2 Theoretical Framework

The $\Lambda_b \to \Lambda \ell^+ \ell^-$ channel proceeds via FCNC $b \to s$ transition at quark level. The effective Hamiltonian describing the electroweak penguin and weak box diagrams related to this transition can be written as :

$$\mathcal{H}_{eff} = \frac{G_F \ \alpha_{em} V_{tb} \ V_{ts}^*}{2\sqrt{2} \ \pi} \Big\{ C_9^{eff} \ \bar{s}\gamma_\mu (1-\gamma_5) b \bar{l} \gamma^\mu l + C_{10} \ \bar{s}\gamma_\mu (1-\gamma_5) b \bar{l} \gamma^\mu \gamma_5 l$$

$$- \ 2m_b \ C_7 \frac{1}{q^2} \ \bar{s} i\sigma_{\mu\nu} q^\nu (1+\gamma_5) b \bar{l} \gamma^\mu l \Big\} \ . \tag{1}$$

To find the amplitude, we need to sandwich this effective Hamiltonian between the initial and final baryon states, i.e., $\langle \Lambda_b(p+q)|\mathcal{H}_{eff}|\Lambda(p)\rangle$. From Eq. (1) we see that in calculation of the $\Lambda_b \to \Lambda \ell^+ \ell^-$ decay amplitude, the matrix elements, $\langle \Lambda_b(p+q)|\bar{b}\gamma_\mu(1-\gamma_5)s|\Lambda(p)\rangle$ and $\langle \Lambda_b(p+q)|\bar{b} i\sigma_{\mu\nu} q^\nu (1+\gamma_5)s|\Lambda(p)\rangle$ are appeared. These matrix elements can be parametrized in terms of the twelve form factors, f_i, g_i, f_i^T and g_i^T in the following manner:

$$\langle \Lambda(p) \mid \bar{s}\gamma_\mu(1-\gamma_5)b \mid \Lambda_b(p+q)\rangle = \bar{u}_\Lambda(p)\Big[\gamma_\mu f_1(Q^2) + i\sigma_{\mu\nu}q^\nu f_2(Q^2) + q^\mu f_3(Q^2)$$
$$- \ \gamma_\mu\gamma_5 g_1(Q^2) - i\sigma_{\mu\nu}\gamma_5 q^\nu g_2(Q^2) - q^\mu \gamma_5 g_3(Q^2)\Big] u_{\Lambda_b}(p+q) \ , \tag{2}$$

and

$$\langle \Lambda(p) \mid \bar{s} i\sigma_{\mu\nu}q^\nu(1+\gamma_5)b \mid \Lambda_b(p+q)\rangle = \bar{u}_\Lambda(p)\Big[\gamma_\mu f_1^T(Q^2) + i\sigma_{\mu\nu}q^\nu f_2^T(Q^2) + q^\mu f_3^T(Q^2)$$
$$+ \ \gamma_\mu\gamma_5 g_1^T(Q^2) + i\sigma_{\mu\nu}\gamma_5 q^\nu g_2^T(Q^2) + q^\mu \gamma_5 g_3^T(Q^2)\Big] u_{\Lambda_b}(p+q) \ , \tag{3}$$

where $Q^2 = -q^2$. For calculation of these form factors we use the QCD sum rules approach. To obtain the sum rules for the form factors in this approach, the following correlation functions, the main objects in this approach, are considered:

$$\Pi_\mu^I(p,q) = i \int d^4x e^{-iqx} \langle 0 \mid T\{J^{\Lambda_b}(0), \bar{b}(x)\gamma_\mu(1-\gamma_5)s(x))\} \mid \Lambda(p)\rangle \ ,$$
$$\Pi_\mu^{II}(p,q) = i \int d^4x e^{-iqx} \langle 0 \mid T\{J^{\Lambda_b}(0), \bar{b}(x) i\sigma_{\mu\nu}q^\nu(1+\gamma_5)s(x)\} \mid \Lambda(p)\rangle \ , \tag{4}$$

where, p represents the Λ's momentum and q is the transferred momentum and the J^{Λ_b} is interpolating current of Λ_b. The most general form of the interpolating current of Λ_b baryon can be written as:

$$J^{\Lambda_b}(x) = \frac{1}{\sqrt{6}}\epsilon_{abc}\Big\{2\Big[(q_1^{aT}(x)Cq_2^b(x))\gamma_5 b^c(x) + \beta(q_1^{aT}(x)C\gamma_5 q_2^b(x))b^c(x)\Big]$$
$$+ \ (q_1^{aT}(x)Cb^b(x))\gamma_5 q_2^c(x) + \beta(q_1^{aT}(x)C\gamma_5 b^b(x))q_2^c(x)$$
$$+ \ (b^{aT}(x)Cq_2^b(x))\gamma_5 q_1^c(x) + \beta(b^{aT}(x)C\gamma_5 q_2^b(x))q_1^c(x)\Big\} \ , \tag{5}$$

where q_1 and q_2 are the u and d quarks, respectively, a, b and c are color indexes and C is the charge conjugation operator. The β is an arbitrary parameter with $\beta = -1$ corresponding to the Ioffe current.

In order to obtain the sum rules for the transition form factors, we will calculate the aforementioned correlation functions in two different ways, namely, physical (phenomenological) and theoretical (QCD) sides and equate these two representations isolating the

ground state through the dispersion relation. Finally, to suppress the contribution of the higher states and continuum, we will apply the Borel transformation and continuum subtraction to both sides of the correlation function and impose the quark hadron duality assumption.

The first step is to calculate the physical side of the correlation functions. Saturating the correlation functions with complete set of the intermediate states with the same quantum numbers as the initial state, for the physical part of the correlation function we obtain,

$$\Pi_\mu^I(p,q) = \sum_s \frac{\langle 0 \mid J^{\Lambda_b}(0) \mid \Lambda_b(p+q,s)\rangle \langle \Lambda_b(p+q,s) \mid \bar{b}\gamma_\mu(1-\gamma_5)s \mid \Lambda(p)\rangle}{m_{\Lambda_b}^2 - (p+q)^2} + \cdots \ , \tag{6}$$

$$\Pi_\mu^{II}(p,q) = \sum_s \frac{\langle 0 \mid J^{\Lambda_b}(0) \mid \Lambda_b(p+q,s)\rangle \langle \Lambda_b(p+q,s) \mid \bar{b}i\sigma_{\mu\nu}q^\nu(1+\gamma_5)s \mid \Lambda(p)\rangle}{m_{\Lambda_b}^2 - (p+q)^2} + \cdots \ , \tag{7}$$

where the dots $\cdots$ represent the contribution of the higher states and continuum. The vacuum to the baryon matrix element of the interpolating current, $\langle 0 \mid J^{\Lambda_b}(0) \mid \Lambda_b(p+q,s)\rangle$ is written in terms of the residue, λ_{Λ_b} as:

$$\langle 0 \mid J^{\Lambda_b}(0) \mid \Lambda_b(p+q,s)\rangle = \lambda_{\Lambda_Q} \bar{u}_{\Lambda_Q}(p+q,s) \ . \tag{8}$$

Putting Eqs. (2), (3) and (8) in Eqs. (6) and (7) and performing summation over spins of the Λ_b baryon using

$$\sum_s u_{\Lambda_b}(p+q,s)\overline{u}_{\Lambda_b}(p+q,s) = \not{p} + \not{q} + m_{\Lambda_b} \ , \tag{9}$$

we get the following expressions for the correlation functions

$$\begin{aligned}\Pi_\mu^I(p,q) &= \lambda_{\Lambda_b}\frac{\not{p}+\not{q}+m_{\Lambda_b}}{m_{\Lambda_b}^2-(p+q)^2}\Big\{\gamma_\mu f_1 - i\sigma_{\mu\nu}q^\nu f_2 + q_\mu f_3 \\ &- \gamma_\mu\gamma_5 g_1 - i\sigma_{\mu\nu}q^\nu\gamma_5 g_2 + q_\mu\gamma_5 g_3\Big\}u_\Lambda(p) \ ,\end{aligned} \tag{10}$$

$$\begin{aligned}\Pi_\mu^{II}(p,q) &= \lambda_{\Lambda_b}\frac{\not{p}+\not{q}+m_{\Lambda_b}}{m_{\Lambda_b}^2-(p+q)^2}\Big\{\gamma_\mu f_1^T - i\sigma_{\mu\nu}q^\nu f_2^T + q^\mu f_3^T \\ &+ \gamma_\mu\gamma_5 g_1^T + i\sigma_{\mu\nu}\gamma_5 q^\nu g_2^T - q^\mu\gamma_5 g_3^T\Big\}u_\Lambda(p) \ .\end{aligned} \tag{11}$$

Using the equation of motion and Eqs. (10) and (11), we get the following final expressions for the phenomenological sides of the correlation functions:

$$\begin{aligned}\Pi_\mu^I(p,q) &= \frac{\lambda_{\Lambda_b}}{m_{\Lambda_b}^2-(p+q)^2}\Big\{2f_1(Q^2)p_\mu + 2f_2(Q^2)p_\mu\not{q} + \Big[f_2(Q^2)+f_3(Q^2)\Big]q_\mu\not{q} \\ &- 2g_1(Q^2)p_\mu\gamma_5 + 2g_2(Q^2)p_\mu\not{q}\gamma_5 + \Big[g_2(Q^2)+g_3(Q^2)\Big]q_\mu\not{q}\gamma_5 \\ &+ \text{other structures}\Big\}u_\Lambda(p) \ ,\end{aligned} \tag{12}$$

$$\Pi_\mu^{II}(p,q) = \frac{\lambda_{\Lambda_b}}{m_{\Lambda_b}^2-(p+q)^2}\Big\{2f_1^T(Q^2)p_\mu + 2f_2^T(Q^2)p_\mu \not{q} + \Big[f_2^T(Q^2)+f_3^T(Q^2)\Big]q_\mu \not{q}$$
$$+ 2g_1^T(Q^2)p_\mu\gamma_5 - 2g_2^T(Q^2)p_\mu \not{q}\gamma_5 - \Big[g_2^T(Q^2)+g_3^T(Q^2)\Big]q_\mu \not{q}\gamma_5$$
$$+ \text{other structures}\Big\}u_\Lambda(p) \ . \tag{13}$$

To compute the form factors or their combinations, f_1, f_2, f_2+f_3, g_1, g_2 and g_2+g_3, we will choose the independent structures p_μ, $p_\mu\not{q}$, $q_\mu\not{q}$, $p_\mu\gamma_5$, $p_\mu\not{q}\gamma_5$, and $q_\mu\not{q}\gamma_5$ from Eq. (12), respectively. The same structures are selected to calculate the form factors or their combinations labeled by T in the second correlation function, Eq. (13).

The next step is to calculate the correlation functions from QCD side in deep Euclidean region where $(p+q)^2 \ll 0$. For this aim, we expend the time ordering products of the interpolating current of the Λ_b and transition currents in the correlation functions (see Eq. (4)) near the light cone, $x^2 \simeq 0$ via operator product expansion, where the short and long distance effects are separated. The former is calculated using QCD perturbation theory, whereas the latter are parameterized in terms of the Λ DA's. Mathematically, this is equivalent to contract out all quark pairs in the time ordering product of the J^{Λ_b} and transition currents via the Wick's theorem. As a result of this procedure, we obtain the following representations of the correlation functions in QCD side:

$$\Pi_\mu^{I} = \frac{-i}{\sqrt{6}}\epsilon^{abc}\int d^4x e^{iqx}\Big\{\Big[2(C)_{\eta\phi}(\gamma_5)_{\rho\beta} + (C)_{\eta\beta}(\gamma_5)_{\rho\phi} + (C)_{\beta\phi}(\gamma_5)_{\eta\rho}\Big]$$
$$+ \beta\Big[2(C\gamma_5)_{\eta\phi}(I)_{\rho\beta} + (C\gamma_5)_{\eta\beta}(I)_{\rho\phi} + (C\gamma_5)_{\beta\phi}(I)_{\eta\rho}\Big]\Big\}\Big[\gamma_\mu(1-\gamma_5)\Big]_{\sigma\theta}$$
$$\times\ S_b(-x)_{\beta\sigma}\langle 0|u_\eta^a(0)s_\theta^b(x)d_\phi^c(0)|\Lambda(p)\rangle \ , \tag{14}$$

$$\Pi_\mu^{II} = \frac{-i}{\sqrt{6}}\epsilon^{abc}\int d^4x e^{iqx}\Big\{\Big[2(C)_{\eta\phi}(\gamma_5)_{\rho\beta} + (C)_{\eta\beta}(\gamma_5)_{\rho\phi} + (C)_{\beta\phi}(\gamma_5)_{\eta\rho}\Big]$$
$$+ \beta\Big[2(C\gamma_5)_{\eta\phi}(I)_{\rho\beta} + (C\gamma_5)_{\eta\beta}(I)_{\rho\phi} + (C\gamma_5)_{\beta\phi}(I)_{\eta\rho}\Big]\Big\}\Big[iq^\nu\sigma_{\mu\nu}(1+\gamma_5)\Big]_{\sigma\theta}$$
$$\times\ S_b(-x)_{\beta\sigma}\langle 0|u_\eta^a(0)s_\theta^b(x)d_\phi^c(0)|\Lambda(p)\rangle \ , \tag{15}$$

The heavy quark propagator, $S_b(x)$ is calculated in [23]:

$$S_b(x) = S_b^{free}(x) - ig_s\int\frac{d^4k}{(2\pi)^4}e^{-ikx}\int_0^1 dv\Big[\frac{\not{k}+m_Q}{(m_Q^2-k^2)^2}G^{\mu\nu}(vx)\sigma_{\mu\nu}$$
$$+ \frac{1}{m_Q^2-k^2}vx_\mu G^{\mu\nu}\gamma_\nu\Big] \ . \tag{16}$$

where,

$$S_b^{free} = \frac{m_b^2}{4\pi^2}\frac{K_1(m_b\sqrt{-x^2})}{\sqrt{-x^2}} - i\frac{m_b^2\not{x}}{4\pi^2x^2}K_2(m_b\sqrt{-x^2}) \ , \tag{17}$$

and K_i are the Bessel functions. The terms proportional to the gluon field strength are contributed mainly to the four and five particle distribution functions [23–27] and expected to be very small in our case, hence when doing calculations, these terms are ignored. The matrix element $\epsilon^{abc}\langle 0|u^a_\eta(0)d^b_\theta(0)s^c_\phi(x)|\Lambda(p)\rangle$ appearing in Eqs. (14,15) represents the Λ's wave functions, which are calculated in [27] and we list them out for the completeness of this paper in the Appendix. Using the Λ wave functions and the expression of the heavy quark propagator, and after performing the Fourier transformation, the final expressions of the correlation functions for both vertexes are found in terms of the Λ DA's in QCD or theoretical side.

In order to obtain the sum rules for the form factors, f_1, f_2, f_3, g_1, g_2, g_3, f_1^T, f_2^T, f_3^T, g_1^T, g_2^T and g_3^T, we equate the coefficients of the corresponding structures from both sides of the correlation functions through the dispersion relations and apply Borel transformation with respect to $(p+q)^2$ to suppress the contribution of the higher states and continuum. The expressions for the sum rules of the form factors are very lengthy, so we will give only extrapolation formulas to explore their dependency on the transferred momentum squared q^2.

The explicit expressions of the sum rules for the form factors depict that to calculate the values of the form factors, we need also the expression of the residue, λ_{Λ_b}. This residue is calculated in [28].

Few words about the relations among the form factors in HQET are in order. In HQET, the number of independent form factors is reduced to two, F_1 and F_2, so the transition matrix element can be parameterized in terms of these two form factors as [28, 29]:

$$\langle \Lambda(p) \mid \bar{s}\Gamma b \mid \Lambda_b(p+q)\rangle = \bar{u}_\Lambda(p)[F_1(Q^2) + \not{v}F_2(Q^2)]\Gamma u_{\Lambda_b}(p+q), \tag{18}$$

Here, Γ refers to any Dirac matrices and $\not{v} = (\not{p}+\not{q})/m_{\Lambda_b}$. Comparing this matrix element with definitions of the form factors in Eqs. (2) and (3), the following relations among the form factors are obtained (see also [30, 31]):

$$\begin{aligned}
f_1 &= g_1 = f_2^T = g_2^T = F_1 + \frac{m_\Lambda}{m_{\Lambda_b}}F_2 \ , \\
f_2 &= g_2 = f_3 = g_3 = \frac{F_2}{m_{\Lambda_b}} \ , \\
f_1^T &= g_1^T = \frac{F_2}{m_{\Lambda_b}}q^2 \ , \\
f_3^T &= -\frac{F_2}{m_{\Lambda_b}}(m_{\Lambda_b} - m_\Lambda) \ , \\
g_3^T &= \frac{F_2}{m_{\Lambda_b}}(m_{\Lambda_b} + m_\Lambda) \ .
\end{aligned} \tag{19}$$

3 Numerical Analysis

This section is devoted to the numerical analysis of the form factors, their extrapolation in terms of the momentum transferred square and calculation of the total decay rate and branching ratio for rare $\Lambda_b \to \Lambda\ell^+\ell^-$ transition in QCD.

Some input parameters used in the numerical calculations are: $\langle\bar{u}u\rangle(1\,GeV) = \langle\bar{d}d\rangle(1\,GeV) = -(0.243\pm0.01)^3\,GeV^3$, $m_0^2(1\,GeV) = (0.8\pm0.2)\,GeV^2$ [32], $m_\Lambda = (1115.683\pm0.006)\,MeV$, $m_{\Lambda_b} = (5620.2\pm1.6)\,MeV$ and $m_b = (4.7\pm0.1)\,GeV$. Sum rules for the form factors depict that the Λ DA's are the main input parameters (see the Appendix). They contain 4 independent parameters which are given as [27]:

$$f_\Lambda = (6.0\pm0.3)\times10^{-3}\ \text{GeV}^2\,, \qquad \lambda_1 = (1.0\pm0.3)\times10^{-2}\ \text{GeV}^2\,,$$
$$|\lambda_2| = (0.83\pm0.05)\times10^{-2}\ \text{GeV}^2\,, \qquad |\lambda_3| = (0.83\pm0.05)\times10^{-2}\ \text{GeV}^2\,. \quad (20)$$

It is well known that, the Wilson coefficient C_9^{eff} receives long distance contributions from J/ψ family, in addition to short distance contributions. In the present work, we do not take into account the long distance effects. From the explicit expressions for the form factors, it is clear that they depend on three auxiliary parameters, continuum threshold s_0, Borel mass parameter M_B^2 and the parameter β entering the most general form of the interpolating current of the Λ_b. The form factors should be independent of these auxiliary parameters. Therefore, we look for working regions for these parameters, where the form factors are practically independent of them. To determine the working region for the Borel mass parameter the procedure is as follows: the lower limit is obtained requiring that the higher states and continuum contributions constitute a small percent of the total dispersion integral. The upper limit of M_B^2 is chosen demanding that the series of the light cone expansion with increasing twist should be convergent. As a result, the common working region of M_B^2 is found to be $15\ GeV^2 \leq M_B^2 \leq 30\ GeV^2$. As an example, we present the dependence of the form factor f_1 on Borel mass parameter, M_B^2 at two fixed values of q^2 in Fig. 1. From this figure it follows that the form factor f_1 exhibits a good stability with respect to the variations of M_B^2. The continuum threshold s_0 is correlated to the first exited state with quantum numbers of the interpolating current of the Λ_b and is not completely arbitrary. Numerical analysis leads to the interval, $(m_{\Lambda_b}+0.3)^2 \leq s_0 \leq (m_{\Lambda_b}+0.5)^2$, where the form factors weakly depend on the continuum threshold. In order to attain the working region for the parameter, β, we look for the variation of the form factors with respect to $\cos\theta$, where $\beta = tan\theta$. After performing numerical calculations, we obtained that in the interval $-0.6 \leq \cos\theta \leq 0.3$ all form factors weakly depend on β. As an example, we show the dependence of the form factor, f_1 on $\cos\theta$ at two fixed values of the q^2 and at $M_B^2 = 22\ GeV^2$ in Fig. 2 . From this figure indeed we see that in the aforementioned region of $\cos\theta$, the form factor f_1 weakly depends on β.

The analysis of the sum rules, as has already been explained above, is based on, so called, the standard procedure, i.e., the continuum threshold s_0 is independent of M_B^2 and q^2. However, in [33], instead of the standard procedure, namely, independence of the s_0 from M_B^2 and q^2, it is assumed that the continuum threshold depends on M_B^2 and q^2 and this leads to large realistic errors. Following [33], in the present work the systematic error is taken to be around 15%.

In calculating the branching ratio of the $\Lambda_b \to \Lambda\ell^+\ell^-$ decay, the dependence of the form factors $f_i(q^2)$, $g_i(q^2)$, $f_i^T(q^2)$, and $g_i^T(q^2)$ on q^2 in the physical region $4m_\ell^2 \leq q^2 \leq (m_{\Lambda_b}-m_\Lambda)^2$ are needed. But unfortunately, sum rules predictions for the form factors are not reliable in the whole physical region. Therefore, in order to obtain the q^2 dependence of the form factors from sum rules we consider a range of q^2 where the correlation function can reliably be calculated. For this aim we choose a region which is approximately 1 GeV below the

	QCD sum rules		
	a	b	m^2_{fit}
f_1	-0.046	0.368	39.10
f_2	0.0046	-0.017	26.37
f_3	0.006	-0.021	22.99
g_1	-0.220	0.538	48.70
g_2	0.005	-0.018	26.93
g_3	0.035	-0.050	24.26
f_2^T	-0.131	0.426	45.70
f_3^T	-0.046	0.102	28.31
g_2^T	-0.369	0.664	59.37
g_3^T	-0.026	-0.075	23.73

Table 1: Parameters appearing in the fit function of the form factors, f_1, f_2, f_3, g_1, g_2, g_3, f_2^T, f_3^T, g_2^T and g_3^T in full theory for $\Lambda_b \to \Lambda \ell^+ \ell^-$. In this Table only central values of the parameters are presented.

perturbative cut, i.e., up to $q^2 \simeq 12\ GeV^2$. To be able to extend the results for the form factors to the whole physical region, we look for a parameterization of the form factors in such a way that, in the region $4m_\ell^2 \leq q^2 \leq 12\ GeV^2$ this parameterization coincides with the sum rules predictions.

The next step is to present the q^2 dependency of the form factors. Our numerical calculations show that the best parameterization for the dependence of the form factors f_1, f_2, f_3, g_1, g_2, g_3, f_2^T, f_3^T, g_2^T and g_3^T on q^2 is as follows:

$$f_i(q^2)[g_i(q^2)] = \frac{a}{\left(1 - \frac{q^2}{m^2_{fit}}\right)} + \frac{b}{\left(1 - \frac{q^2}{m^2_{fit}}\right)^2}\ , \tag{21}$$

where the fit parameters $a,\ b$ and m^2_{fit} in full theory are given in Table 1. On the other hand, we find that the best fit for the form factors f_1^T and g_1^T is of the following form,

$$f_1^T(q^2)[g_1^T(q^2)] = \frac{c}{\left(1 - \frac{q^2}{m'^2_{fit}}\right)} - \frac{c}{\left(1 - \frac{q^2}{m''^2_{fit}}\right)^2}\ . \tag{22}$$

The results for the parameters c, m'^2_{fit} and m''^2_{fit} are presented in Table 2. In extraction of the values of the fit parameters presented in both Tables 1 and 2, the values of the continuum threshold, $s_0 = 35\ GeV^2$, Borel mass parameter, $M_B^2 = 22\ GeV^2$ and $\cos\theta = 0.2$ have been used.

	QCD sum rules		
	c	m'^2_{fit}	m''^2_{fit}
f_1^T	-1.191	23.81	59.96
g_1^T	-0.653	24.15	48.52

Table 2: Parameters appearing in the fit function of the form factors f_1^T and g_1^T in full theory for $\Lambda_b \to \Lambda \ell^+ \ell^-$.

The values of form factors at $q^2 = 0$ are also presented in Table 3. In this table we also present the numerical results obtained from HQET, using the values for the form factors $F_1(0) = 0.462$ and $F_2 = -0.077$ predicted in [17], and relations in Eq. (19) at HQET limit. The errors in the values of the form factors at $q^2 = 0$ are due to the uncertainties coming from M_B^2, s_0, the parameter β, errors in the input parameters, as well as from the systematic errors. From this Table we see that, the predictions of the HQET on the form factors are changed more than 40% for the form factors $f_1(0)$, $g_1(0)$, $f_2^T(0)$, and $g_1^T(0)$, while the results of both approaches are very close to each other for the remaining form factors.

	Present work	HQET ([13])
$f_1(0)$	0.322 ± 0.112	0.446
$f_2(0)$	-0.011 ± 0.004	-0.013
$f_3(0)$	-0.015 ± 0.005	-0.013
$g_1(0)$	0.318 ± 0.110	0.446
$g_2(0)$	-0.013 ± 0.004	-0.013
$g_3(0)$	-0.014 ± 0.005	-0.013
$f_1^T(0)$	0 ± 0.0	0.0
$f_2^T(0)$	0.295 ± 0.105	0.446
$f_3^T(0)$	0.056 ± 0.018	0.061
$g_1^T(0)$	0 ± 0.0	0.0
$g_2^T(0)$	0.294 ± 0.105	0.446
$g_3^T(0)$	-0.101 ± 0.035	-0.092

Table 3: The values of the form factors at $q^2 = 0$ for $\Lambda_b \to \Lambda \ell^+ \ell^-$.

The final task is to calculate the total decay rate of the $\Lambda_b \to \Lambda \ell^+ \ell^-$ transition in the

whole physical region, $4m_\ell^2 \leq q^2 \leq (m_{\Lambda_b} - m_\Lambda)^2$. The differential decay rate is obtained as:

$$\frac{d\Gamma}{ds} = \frac{G^2\alpha_{em}^2 m_{\Lambda_b}}{8192\pi^5}|V_{tb}V_{ts}^*|^2 v\sqrt{\lambda}\left[\Theta(s) + \frac{1}{3}\Delta(s)\right], \tag{23}$$

where $s = q^2/m_{\Lambda_b}^2$, $r = m_\Lambda^2/m_{\Lambda_b}^2$, $\lambda = \lambda(1,r,s) = 1+r^2+s^2-2r-2s-2rs$, $G_F = 1.17\times10^{-5}$ GeV^{-2} is the Fermi coupling constant and $v = \sqrt{1-\frac{4m_\ell^2}{q^2}}$ is the lepton velocity. For the element of the CKM matrix $\mid V_{tb}V_{ts}^* \mid = 0.041$ has been used [34]. The functions $\Theta(s)$ and $\Delta(s)$ are given as:

$$\begin{aligned}
\Theta(s) =\ & 32m_\ell^2 m_{\Lambda_b}^4 s(1+r-s)\left(|D_3|^2+|E_3|^2\right) \\
&+ 64m_\ell^2 m_{\Lambda_b}^3(1-r-s)\,\mathrm{Re}[D_1^*E_3 + D_3E_1^*] \\
&+ 64m_{\Lambda_b}^2\sqrt{r}(6m_\ell^2 - m_{\Lambda_b}^2 s)\mathrm{Re}[D_1^*E_1] \\
&+ 64m_\ell^2 m_{\Lambda_b}^3\sqrt{r}\Big(2m_{\Lambda_b}s\mathrm{Re}[D_3^*E_3] + (1-r+s)\mathrm{Re}[D_1^*D_3 + E_1^*E_3]\Big) \\
&+ 32m_{\Lambda_b}^2(2m_\ell^2 + m_{\Lambda_b}^2 s)\Big\{(1-r+s)m_{\Lambda_b}\sqrt{r}\,\mathrm{Re}[A_1^*A_2 + B_1^*B_2] \\
&- m_{\Lambda_b}(1-r-s)\,\mathrm{Re}[A_1^*B_2 + A_2^*B_1] - 2\sqrt{r}\Big(\mathrm{Re}[A_1^*B_1] + m_{\Lambda_b}^2 s\,\mathrm{Re}[A_2^*B_2]\Big)\Big\} \\
&+ 8m_{\Lambda_b}^2\Big\{4m_\ell^2(1+r-s) + m_{\Lambda_b}^2\Big[(1-r)^2 - s^2\Big]\Big\}\left(|A_1|^2+|B_1|^2\right) \\
&+ 8m_{\Lambda_b}^4\Big\{4m_\ell^2\Big[\lambda + (1+r-s)s\Big] + m_{\Lambda_b}^2 s\Big[(1-r)^2 - s^2\Big]\Big\}\left(|A_2|^2+|B_2|^2\right) \\
&- 8m_{\Lambda_b}^2\Big\{4m_\ell^2(1+r-s) - m_{\Lambda_b}^2\Big[(1-r)^2 - s^2\Big]\Big\}\left(|D_1|^2+|E_1|^2\right) \\
&+ 8m_{\Lambda_b}^5 sv^2\Big\{-8m_{\Lambda_b}s\sqrt{r}\,\mathrm{Re}[D_2^*E_2] + 4(1-r+s)\sqrt{r}\,\mathrm{Re}[D_1^*D_2 + E_1^*E_2] \\
&- 4(1-r-s)\,\mathrm{Re}[D_1^*E_2 + D_2^*E_1] + m_{\Lambda_b}\Big[(1-r)^2 - s^2\Big]\left(|D_2|^2+|E_2|^2\right)\Big\},
\end{aligned} \tag{24}$$

$$\begin{aligned}
\Delta(s) =\ & -8m_{\Lambda_b}^4 v^2\lambda\left(|A_1|^2+|B_1|^2+|D_1|^2+|E_1|^2\right) \\
&+ 8m_{\Lambda_b}^6 sv^2\lambda\Big(|A_2|^2+|B_2|^2+|D_2|^2+|E_2|^2\Big),
\end{aligned} \tag{25}$$

where

$$\begin{aligned}
A_1 &= \frac{1}{q^2}\left(f_1^T + g_1^T\right)(-2m_bC_7) + (f_1 - g_1)\,C_9^{eff} \\
A_2 &= A_1\,(1\to 2)\ , \\
A_3 &= A_1\,(1\to 3)\ , \\
B_1 &= A_1\left(g_1 \to -g_1;\ g_1^T \to -g_1^T\right)\ , \\
B_2 &= B_1\,(1\to 2)\ , \\
B_3 &= B_1\,(1\to 3)\ , \\
D_1 &= (f_1 - g_1)\,C_{10}\ , \\
D_2 &= D_1\,(1\to 2)\ ,
\end{aligned} \tag{26}$$

$$
\begin{aligned}
D_3 &= D_1\left(1 \to 3\right) \ , \\
E_1 &= D_1\left(g_1 \to -g_1\right) \ , \\
E_2 &= E_1\left(1 \to 2\right) \ , \\
E_3 &= E_1\left(1 \to 3\right) \ .
\end{aligned} \tag{27}
$$

Integrating the differential decay rate on s in the whole physical region $4m_\ell^2/m_{\Lambda_b}^2 \leq s \leq (1-\sqrt{r})^2$ and using the life time of the Λ_b baryon, $\tau_{\Lambda_b} = 1.383 \times 10^{-12}\ s$ [34], we obtain the results for the branching ratio which are presented in Table 4.

	Present work	HQET([19])
$Br(\Lambda_b \to \Lambda e^+ e^-)$	$(4.6 \pm 1.6) \times 10^{-6}$	$(2.23 \div 3.34) \times 10^{-6}$
$Br(\Lambda_b \to \Lambda \mu^+ \mu^-)$	$(4.0 \pm 1.2) \times 10^{-6}$	$(2.08 \div 3.19) \times 10^{-6}$
$Br(\Lambda_b \to \Lambda \tau^+ \tau^-)$	$(0.8 \pm 0.3) \times 10^{-6}$	$(0.179 \div 0.276) \times 10^{-6}$

Table 4: Values of the Branching ratio for $\Lambda_b \to \Lambda\ \ell^+\ell^-$ in full theory and HQET for different leptons .

In this Table we also present the values of the branching ratio obtained in HQET [19]. Comparing the results of both approaches, we see that our predictions on the branching ratios for the $\Lambda_b \to \Lambda e^+ e^-$, $\Lambda_b \to \Lambda \mu^+ \mu^-$ channels are larger approximately by a factor of two than the ones predicted by the HQET, while for the $\Lambda_b \to \Lambda \tau^+ \tau^-$ channel our prediction is four times larger than the result of the HQET. Since $10^{10} \div 10^{11}$ pairs are expected to be produced per year at LHCb [35], the results presented in Table–4 show that detectability of $\Lambda_b \to \Lambda \ell^+ \ell^-$ $(\ell = e, \mu, \tau)$ decays in this machine is quite high.

In conclusion, we calculate all twelve form factors responsible for the $\Lambda_b \to \Lambda \ell^+ \ell^-$ decay within light cone sum rules. It is obtained the maximum difference between our results and HQET predictions on the form factors is about 40%. Using the parametrization for the form factors, the branching ratio of the $\Lambda_b \to \Lambda \ell^+ \ell^-$ decay is estimated, and the result we obtain allows us to conclude that the delectability of this decay at LHCb is quite high.

References

[1] M. Mattson et al., (SELEX Collaboration), Phys. Rev. Lett. 89, 112001 (2002).

[2] T. Aaltonen et al., (CDF Collaboration), Phys. Rev. Lett. 99, 052002 (2007); Phys. Rev. Lett. 99, 202001 (2007).

[3] R. Chistov et al., (Belle Collaboration), Phys. Rev. Lett. 97, 162001 (2006).

[4] A. Ocherashvili et al., (SELEX Collaboration), Phys. Lett. B 628, 18 (2005).

[5] V. Abazov et al., (D0 Collaboration), Phys. Rev. Lett. 99, 052001 (2007); Phys. Rev. Lett. 101, 232002 (2008).

[6] D. Acosta et al., (CDF Collaboration), Phys. Rev. Lett. 96, 202001 (2006).

[7] B. Aubert et al., (BABAR Collaboration), Phys. Rev. Lett. 97, 232001 (2006); Phys. Rev. Lett. 99, 062001 (2007); Phys. Rev. D 77, 012002 (2008).

[8] E. Solovieva et al., (Belle Collaboration), Phys. Lett. B 672, 1 (2009).

[9] T. M. Aliev, A. Ozpineci, M. Savci, Nucl.Phys. B 649 (2003) 168.

[10] G. Buchalla, G. Hiller and G. Isidori, Phys. Rev. D 63 (2000) 014015.

[11] C. Bird, P. Jackson, R. Kowalewski, M. Pospelov, Phys. Rev. Lett. 93 (2004) 201803.

[12] R. S. Marques de Carvalho, F. S. Navarra1, M. Nielsen, E. Ferreira, H. G. Dosch, Phys. Rev. D 60, 034009 (1999).

[13] C. -S. Huang, C. -F. Qiao, H. -G. Yan, Phys. Lett. B 437 (1998) 403.

[14] A. Datta, arXiv:hep-ph/9504429.

[15] Yu-Ming Wang, Ying Li, Cai-Dian Lu, Eur. Phys. J. C 59, 861 (2009).

[16] Yu-Ming Wang, Yue-Long Shen, Cai-Dian Lu, Phys. Rev. D 80, 074012 (2009).

[17] C. S. Huang, H. G. Yan, Phys. Rev. D 59, 114022 (1999).

[18] C. –H. Chen, C. Q. Ceng, Phys. Lett. B 516, 327 (2001).

[19] C. –H. Chen, C. Q. Ceng, Phys. Rev. D 64, 074001 (2001).

[20] K. Azizi, M. Bayar, A. Ozpineci, Y. Sarac, Phys. Rev. D 80, 036007 (2009).

[21] K. Azizi, M. Bayar, Y. Sarac, H. Sundu, Phys. Rev. D 80, 096007 (2009).

[22] K. Azizi, M. Bayar, M. T. Zeyrek, arXiv:0910.4521 [hep-ph].

[23] I. I. Balitsky, V. M. Braun, Nucl. Phys. B311 (1989) 541.

[24] V. M. Braun, A. Lenz, N. Mahnke, E. Stein, Phys. Rev. D 65 (2002) 074011.

[25] V. M. Braun, A. Lenz, M. Wittmann, Phys. Rev. D 73 (2006) 094019; A. Lenz, M. Wittmann and E. Stein, Phys. Lett. B 581 (2004) 199.

[26] V. Braun, R. J. Fries, N. Mahnke and E. Stein, Nucl. Phys. B 589 (2000) 381.

[27] Y. L. Liu, M. Q. Huang, Nucl. Phys. A 821, 80 (2009).

[28] T. M. Aliev, A. Ozpineci, M. Savci, Phys. Rev. D 65 (2002) 115002.

[29] T. Mannel, W. Roberts and Z. Ryzak, Nucl. Phys. B355 (1991) 38.

[30] C. H. Chen, C. Q. Geng, Phys. Rev. D 63 (2001) 054005; Phys. Rev. D 63 (2001) 114024; Phys. Rev. D 64 (2001) 074001.

[31] T. M. Aliev, A. Ozpineci, M. Savci, C. Yuce , Phys. Lett. B 542 (2002) 229.

[32] B. L. Ioffe, Prog. Part. Nucl. Phys. 56, 232 (2006).

[33] W. Lucha, D. Melikhov and S. Simula, Phys. Rev. D 79, 0960011 (2009).

[34] C. Amsler et al. [Particle Data Group], Phys. Lett. B 667, 1 (2008).

[35] N. H. Harnew, Proc. of Heavy Flavors 8, (Southampton, 1999).

Appendix

In this Appendix, the general decomposition of the matrix element, $\epsilon^{abc}\langle 0|u^a_\eta(0)s^b_\theta(x)d^c_\phi(0)|\Lambda(p)\rangle$ entering Eqs. (14,15) as well as the Λ DA's are given [27]:

$$
\begin{aligned}
&4\langle 0|\epsilon^{abc}u^a_\alpha(a_1x)s^b_\beta(a_2x)d^c_\gamma(a_3x)|\Lambda(p)\rangle \\
&= \mathcal{S}_1 m_\Lambda C_{\alpha\beta}(\gamma_5\Lambda)_\gamma + \mathcal{S}_2 m^2_\Lambda C_{\alpha\beta}(\not{x}\gamma_5\Lambda)_\gamma \\
&+ \mathcal{P}_1 m_\Lambda(\gamma_5 C)_{\alpha\beta}\Lambda_\gamma + \mathcal{P}_2 m^2_\Lambda(\gamma_5 C)_{\alpha\beta}(\not{x}\Lambda)_\gamma + (\mathcal{V}_1 + \frac{x^2m^2_\Lambda}{4}\mathcal{V}^M_1)(\not{p}C)_{\alpha\beta}(\gamma_5\Lambda)_\gamma \\
&+ \mathcal{V}_2 m_\Lambda(\not{p}C)_{\alpha\beta}(\not{x}\gamma_5\Lambda)_\gamma + \mathcal{V}_3 m_\Lambda(\gamma_\mu C)_{\alpha\beta}(\gamma^\mu\gamma_5\Lambda)_\gamma + \mathcal{V}_4 m^2_\Lambda(\not{x}C)_{\alpha\beta}(\gamma_5\Lambda)_\gamma \\
&+ \mathcal{V}_5 m^2_\Lambda(\gamma_\mu C)_{\alpha\beta}(i\sigma^{\mu\nu}x_\nu\gamma_5\Lambda)_\gamma + \mathcal{V}_6 m^3_\Lambda(\not{x}C)_{\alpha\beta}(\not{x}\gamma_5\Lambda)_\gamma + (\mathcal{A}_1 \\
&+ \frac{x^2m^2_\Lambda}{4}\mathcal{A}^M_1)(\not{p}\gamma_5 C)_{\alpha\beta}\Lambda_\gamma + \mathcal{A}_2 m_\Lambda(\not{p}\gamma_5 C)_{\alpha\beta}(\not{x}\Lambda)_\gamma + \mathcal{A}_3 m_\Lambda(\gamma_\mu\gamma_5 C)_{\alpha\beta}(\gamma^\mu\Lambda)_\gamma \\
&+ \mathcal{A}_4 m^2_\Lambda(\not{x}\gamma_5 C)_{\alpha\beta}\Lambda_\gamma + \mathcal{A}_5 m^2_\Lambda(\gamma_\mu\gamma_5 C)_{\alpha\beta}(i\sigma^{\mu\nu}x_\nu\Lambda)_\gamma + \mathcal{A}_6 m^3_\Lambda(\not{x}\gamma_5 C)_{\alpha\beta}(\not{x}\Lambda)_\gamma \\
&+ (\mathcal{T}_1 + \frac{x^2m^2_\Lambda}{4}\mathcal{T}^M_1)(p^\nu i\sigma_{\mu\nu}C)_{\alpha\beta}(\gamma^\mu\gamma_5\Lambda)_\gamma + \mathcal{T}_2 m_\Lambda(x^\mu p^\nu i\sigma_{\mu\nu}C)_{\alpha\beta}(\gamma_5\Lambda)_\gamma \\
&+ \mathcal{T}_3 m_\Lambda(\sigma_{\mu\nu}C)_{\alpha\beta}(\sigma^{\mu\nu}\gamma_5\Lambda)_\gamma + \mathcal{T}_4 m_\Lambda(p^\nu\sigma_{\mu\nu}C)_{\alpha\beta}(\sigma^{\mu\rho}x_\rho\gamma_5\Lambda)_\gamma \\
&+ \mathcal{T}_5 m^2_\Lambda(x^\nu i\sigma_{\mu\nu}C)_{\alpha\beta}(\gamma^\mu\gamma_5\Lambda)_\gamma + \mathcal{T}_6 m^2_\Lambda(x^\mu p^\nu i\sigma_{\mu\nu}C)_{\alpha\beta}(\not{x}\gamma_5\Lambda)_\gamma \\
&+ \mathcal{T}_7 m^2_\Lambda(\sigma_{\mu\nu}C)_{\alpha\beta}(\sigma^{\mu\nu}\not{x}\gamma_5\Lambda)_\gamma + \mathcal{T}_8 m^3_\Lambda(x^\nu\sigma_{\mu\nu}C)_{\alpha\beta}(\sigma^{\mu\rho}x_\rho\gamma_5\Lambda)_\gamma \ . \qquad (A.1)
\end{aligned}
$$

The calligraphic functions in the above expression have not definite twists but they can be written in terms of the Lambda distribution amplitudes (DA's) with definite and increasing twists via the scalar product px and the parameters a_i, $i = 1, 2, 3$. The explicit expressions for scalar, pseudo-scalar, vector, axial vector and tensor DA's for Lambda are given in Tables 5, 6, 7, 8 and 9, respectively.

$\mathcal{S}_1 = S_1$
$2px\mathcal{S}_2 = S_1 - S_2$

Table 5: Relations between the calligraphic functions and Lambda scalar DA's.

$\mathcal{P}_1 = P_1$
$2px\mathcal{P}_2 = P_1 - P_2$

Table 6: Relations between the calligraphic functions and Lambda pseudo-scalar DA's.

Every distribution amplitude $F(a_ipx)$= S_i, P_i, V_i, A_i, T_i can be represented as:

$$F(a_ipx) = \int dx_1dx_2dx_3\delta(x_1+x_2+x_3-1)e^{ipx\Sigma_i x_i a_i}F(x_i) \ . \qquad (A.2)$$

where, x_i with $i = 1,\ 2$ and 3 are longitudinal momentum fractions carried by the participating quarks.

$\mathcal{V}_1 = V_1$
$2px\mathcal{V}_2 = V_1 - V_2 - V_3$
$2\mathcal{V}_3 = V_3$
$4px\mathcal{V}_4 = -2V_1 + V_3 + V_4 + 2V_5$
$4px\mathcal{V}_5 = V_4 - V_3$
$4(px)^2\mathcal{V}_6 = -V_1 + V_2 + V_3 + V_4 + V_5 - V_6$

Table 7: Relations between the calligraphic functions and Lambda vector DA's.

$\mathcal{A}_1 = A_1$
$2px\mathcal{A}_2 = -A_1 + A_2 - A_3$
$2\mathcal{A}_3 = A_3$
$4px\mathcal{A}_4 = -2A_1 - A_3 - A_4 + 2A_5$
$4px\mathcal{A}_5 = A_3 - A_4$
$4(px)^2\mathcal{A}_6 = A_1 - A_2 + A_3 + A_4 - A_5 + A_6$

Table 8: Relations between the calligraphic functions and Lambda axial vector DA's.

The explicit expressions for the Λ DA's up to twist 6 are given as: twist-3 DA's:

$$\begin{aligned} &V_1(x_i) = 0 \ , && A_1(x_i) = -120x_1x_2x_3\phi_3^0 \ , \\ &T_1(x_i) = 0 \ . \end{aligned} \tag{A.3}$$

twist-4 DA's:

$$\begin{aligned} &S_1(x_i) = 6x_3(1-x_3)(\xi_4^0 + \xi_4^{'0}) \ , && P_1(x_i) = 6(1-x_3)(\xi_4^0 - \xi_4^{'0}) \ , \\ &V_2(x_i) = 0 \ , && A_2(x_i) = -24x_1x_2\phi_4^0 \ , \\ &V_3(x_i) = 12(x_1-x_2)x_3\psi_4^0 \ , && A_3(x_i) = -12x_3(1-x_3)\psi_4^0 \ , \\ &T_2(x_i) = 0 \ , && T_3(x_i) = 6(x_2-x_1)x_3(-\xi_4^0 + \xi_4^{'0}) \ , \\ &T_7(x_i) = -6(x_1-x_2)x_3(\xi_4^0 + \xi_4^{'0}) \ . \end{aligned} \tag{A.4}$$

Ttwist-5 DA's:

$$\begin{aligned} &S_2(x_i) = \frac{3}{2}(x_1+x_2)(\xi_5^0 + \xi_5^{'0}) \ , && P_2(x_i) = \frac{3}{2}(x_1+x_2)(\xi_5^0 - \xi_5^{'0}) \ , \\ &V_4(x_i) = 3(x_2-x_1)\psi_5^0 \ , && A_4(x_i) = -3(1-x_3)\psi_5^0 \ , \\ &V_5(x_i) = 0 \ , && A_5(x_i) = -6x_3\phi_5^0 \ , \\ &T_4(x_i) = -\frac{3}{2}(x_1-x_2)(\xi_5^0 + \xi_5^{'0}) \ , && T_5(x_i) = 0 \ , \\ &T_8(x_i) = -\frac{3}{2}(x_1-x_2)(\xi_5^0 - \xi_5^{'0}) \ . \end{aligned} \tag{A.5}$$

and twist-6 DA's:

$$\begin{aligned} &V_6(x_i) = 0 \ , && A_6(x_i) = -2\phi_6^0 \ , \\ &T_6(x_i) = 0 \ . \end{aligned} \tag{A.6}$$

$\mathcal{T}_1 = T_1$
$2px\mathcal{T}_2 = T_1 + T_2 - 2T_3$
$2\mathcal{T}_3 = T_7$
$2px\mathcal{T}_4 = T_1 - T_2 - 2T_7$
$2px\mathcal{T}_5 = -T_1 + T_5 + 2T_8$
$4(px)^2\mathcal{T}_6 = 2T_2 - 2T_3 - 2T_4 + 2T_5 + 2T_7 + 2T_8$
$4px\mathcal{T}_7 = T_7 - T_8$
$4(px)^2\mathcal{T}_8 = -T_1 + T_2 + T_5 - T_6 + 2T_7 + 2T_8$

Table 9: Relations between the calligraphic functions and Lambda tensor DA's.

The following functions are encountered to the above amplitudes and they can be defined in terms of the 4 independent parameters, namely f_Λ, λ_1, λ_2 and λ_3:

$$\begin{aligned}
&\phi_3^0 = \phi_6^0 = -f_\Lambda \ , && \phi_4^0 = \phi_5^0 = -\frac{1}{2}(f_\Lambda + \lambda_1) \ , \\
&\psi_4^0 = \psi_5^0 = \frac{1}{2}(f_\Lambda - \lambda_1) \ , && \xi_4^0 = \xi_5^0 = \lambda_2 + \lambda_3 \ , \\
&\xi_4^{\prime 0} = \xi_5^{\prime 0} = \lambda_3 - \lambda_2 \ . && (A.7)
\end{aligned}$$

Figure 1: The dependence of form factor, f_1 on Borel mass parameter at two fixed values of the q^2, and at $s_0 = 35\ GeV^2$ and $\beta = 5$.

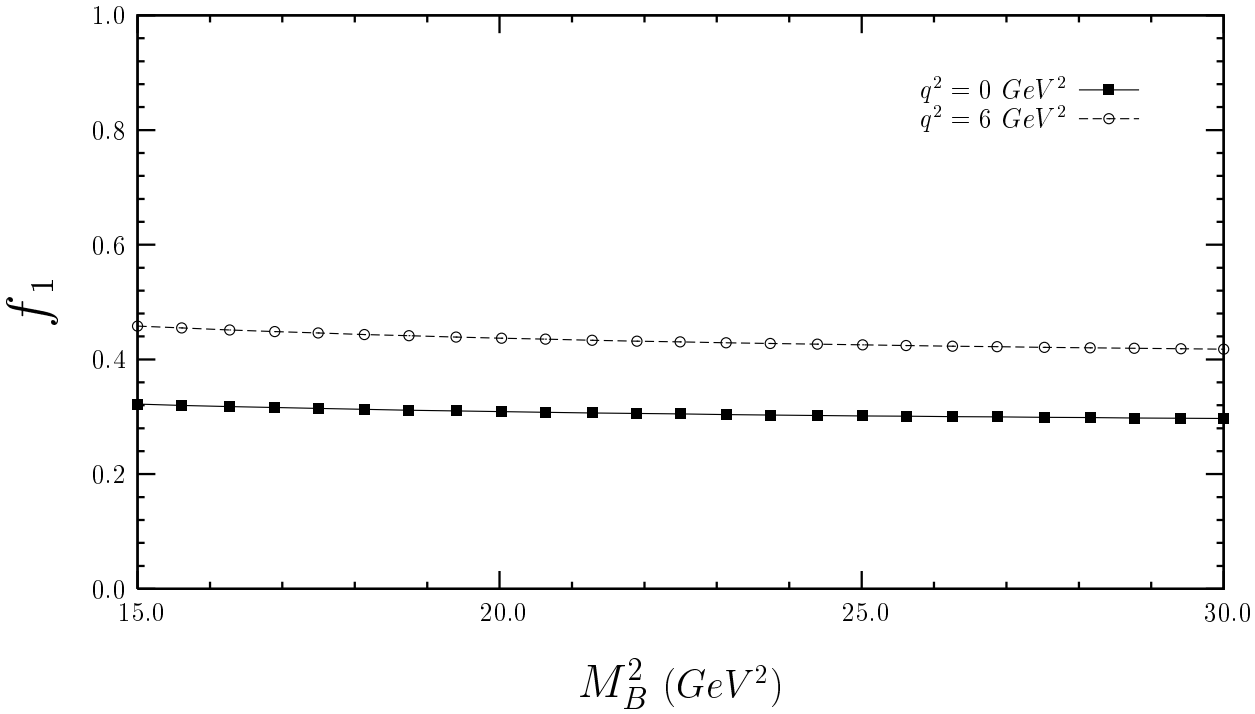

Figure 2: The dependence of form factor, f_1 on $\cos\theta$ parameter at two fixed values of the q^2, and at $s_0 = 35\ GeV^2$ and $M_B^2 = 22\ GeV^2$.